JOURNAL OF GEOPHYSICAL RESEARCH, VOL. 115, C05001, doi:10.1029/2009JC005596, 2010

Physical controls on the seasonal migration of the North Pacific transition zone chlorophyll front

Jennifer M. Ayers[1] and M. Susan Lozier[1]

Received 24 June 2009; revised 10 September 2009; accepted 27 October 2009; published 4 May 2010.

[1] The large seasonal migration of the transition zone chlorophyll front (TZCF) is of interest because a number of marine fauna, both commercial and endangered, appear to track it. Herein we examine the physical dynamics driving this seasonal migration of the TZCF. Vertical processes, traditionally viewed as controlling the dynamical supply of nutrients to surface waters, prove insufficient to explain seasonal variations in nutrient supply to the transition zone. Instead, we find that the horizontal Ekman transport of nutrients from higher latitudes drives the TZCF's southward migration. The estimated horizontal transport of nitrate supports up to 40% of new primary productivity in the region annually and nearly all of new primary productivity in the winter. The significance of horizontal advection to the North Pacific transition zone supports revising the paradigm that nutrients are supplied to surface waters from below.

Citation: Ayers, J. M., and M. S. Lozier (2010), Physical controls on the seasonal migration of the North Pacific transition zone chlorophyll front, *J. Geophys. Res.*, *115*, C05001, doi:10.1029/2009JC005596.

1. Introduction and Background

[2] The North Pacific transition zone (NPTZ) provides habitat for a large number of migratory marine megafauna between California and Japan, including albacore and bluefin tuna, loggerhead and leatherback turtles, black-footed and laysan albatross, northern fur seals, elephant seals, and salmon sharks [*Inagake et al.*, 2001; *Polovina et al.*, 2000, 2001, 2004; *Nichols et al.*, 2000; *Seki*, 2005; *Shaffer et al.*, 2005; *Ream et al.*, 2005; *Simmons et al.*, 2007; *Weng et al.*, 2005]. Biologists have correlated some of these marine fauna pathways with the transition zone chlorophyll front (TZCF), a sharp gradient in sea surface chlorophyll that shifts seasonally north and south through the NPTZ (Figure 1). The nature of the association between migratory animals and the chlorophyll front, however, remains poorly understood. More fundamentally, the dynamics driving the seasonal shift of the TZCF itself are yet to be explained. This paper investigates the physical dynamics forcing the transition zone chlorophyll front throughout the seasonal cycle, with the aim of providing a foundation for subsequent investigations into the association of marine migration routes and the TZCF.

[3] The transition zone chlorophyll front is a permanent gradient in sea surface color that persists zonally across the North Pacific basin, with higher chlorophyll to the north of the front and lower chlorophyll to the south. The TZCF lies approximately within the North Pacific transition zone, the oceanographic region between the subarctic frontal zone and subtropical frontal zone, found at climatological mean positions of 42°N and 32°N, respectively [*Roden*, 1991]. *Polovina et al.* [2001] operationally defined the TZCF as the position of the 0.2 mg m^{-3} chlorophyll *a* contour, corresponding generally to the region of the sharpest chlorophyll gradient. The TZCF shows a strong seasonal signal, shifting latitudinally by about 10° through the year. The chlorophyll front is at its southernmost in winter, around 30°N, and its northernmost in summer, around 40°N. Figure 1 shows the location of the TZCF in February (Figure 1a), May (Figure 1b), August (Figure 1c), and November (Figure 1d). The dynamics of these four months are representative of the seasonal dynamics and as such are used in Figures 1–3 and 5.

[4] Though past studies have shown that migration routes of marine fauna may covary with the seasonally varying latitude of the TZCF, the reason behind this correlation is unclear. Polovina *et al.* link Albacore tuna and loggerhead turtle tracks to the TZCF [*Polovina et al.*, 2000, 2001], but do not propose that these higher trophic level predators actively seek primary productivity. Instead, *Polovina et al.* [2001] posit that the TZCF may coincide with a convergent front along which prey species for tuna and turtles are aggregated. However, the existence of a strong chlorophyll feature in a convergence zone is difficult to reconcile with traditional views on primary productivity: divergent waters support primary productivity through upwelling of nutrient-rich waters from below, while convergent waters are downwelling and generally oligotrophic [*Reid*, 1962]. Untangling these seemingly contradictory associations: top predators with chlorophyll, and chlorophyll with convergent waters, requires first understanding the dynamics of the TZCF itself.

[1]Department of Earth and Ocean Sciences, Nicholas School of the Environment, Duke University, Durham, North Carolina, USA.

0148-0227/10/2009JC005596

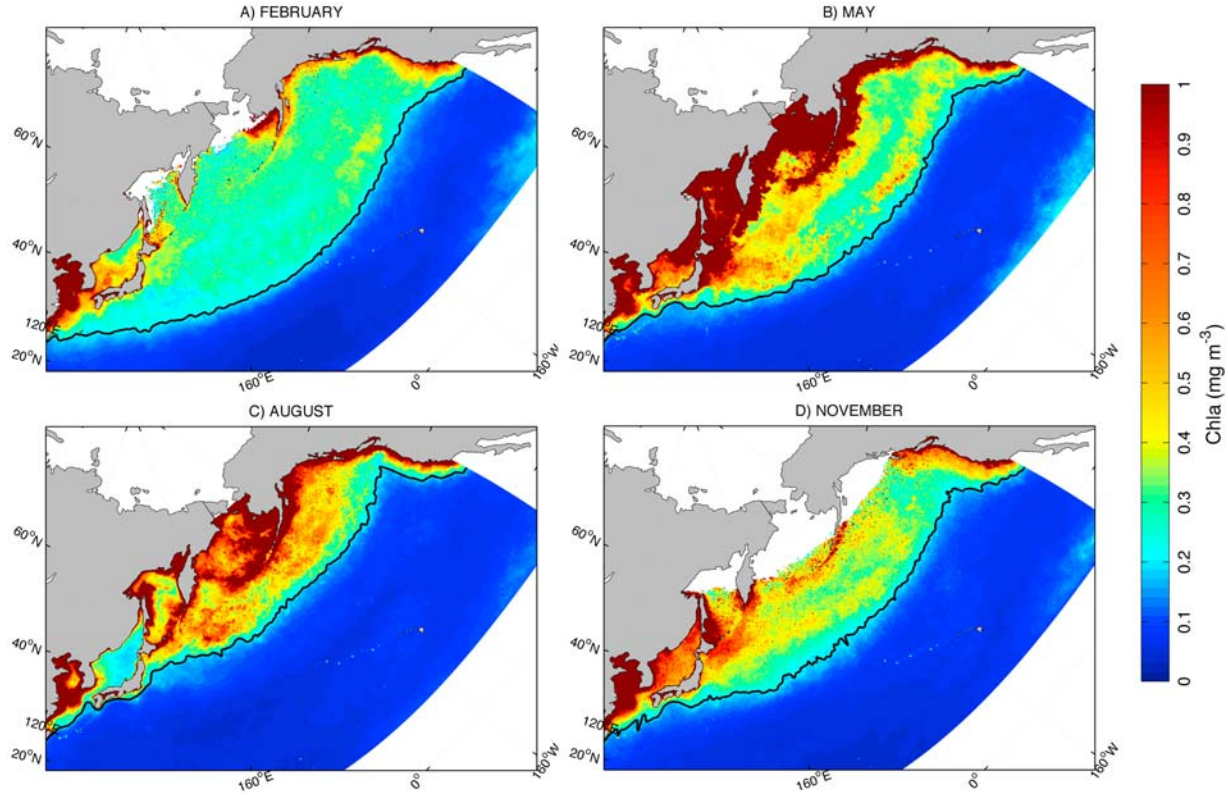

Figure 1. Seasonal latitudinal shift of the TZCF (black line), as shown by 4 months representative of the seasons: (a) February, (b) May, (c) August, and (d) November. The TZCF, defined as the 0.2 mg m^{-3} chlorophyll *a* contour, is overlain on a background of monthly climatological chlorophyll values (mg m^{-3}). Chlorophyll data are 9 km NASA Sea-viewing Wide Field-of-view Sensor (SeaWiFS) from August 1999 to December 2008.

[5] Several studies have investigated the low-latitude position of the wintertime TZCF. Two model studies propose that increased wintertime vertical mixing results in a more southerly TZCF through enhanced nutrient supply [*Glover et al.*, 1994; *Chai et al.*, 2003]. *Chai et al.* [2003] also suggest that the seasonal migration pattern is due to the expansion and contraction of the subarctic and subtropical gyres. In a subsequent study, *Bograd et al.* [2004] found that the winter TZCF position sits atop the region of maximum negative wind stress curl in the subtropical gyre, implying that equatorward advection of nutrient-rich waters from the subarctic gyre plays a role in determining the wintertime TZCF location. This paper considers these proposed drivers for the winter TZCF, as well as examines physical forcing for the TZCF location throughout the rest of the year.

[6] Herein we investigate the physical oceanographic dynamics associated with the large seasonal shift of the transition zone chlorophyll front. Section 2 discusses possible forcing mechanisms for the TZCF: seasonal migration of the gyre-gyre boundary, vertical mixing, and horizontal advection of nutrients. In section 3 we quantify the relative importance of nutrient sources to the TZCF, and in section 4 we discuss the contribution of these nutrient sources to the support of new production. We conclude with a summary of our model for physical controls of the TZCF.

2. Physical Drivers of the Seasonal TZCF

2.1. Gyre-Gyre Boundary

[7] The contrast between the upwelling nature of the subpolar gyre and the downwelling nature of the subtropical gyre creates strong differences in nutrient supply to surface waters in the North Pacific. Upwelling creates surface nitrate values as high as 30 mmol m^{-3} in the subpolar gyre, while downwelling removes nitrate to concentrations below 0.2 mmol m^{-3} in the center of the subtropical gyre (National Oceanographic Data Center World Ocean Atlas 2005 [*Garcia et al.*, 2006, hereafter WOA05]). Correspondingly, we consistently see relatively high chlorophyll in the subpolar gyre and relatively low chlorophyll in the oligotrophic subtropical gyre (Figure 1).

[8] Several studies give us reason to expect that the dynamical boundary between the subpolar and subtropical gyres, and in particular the strong Kuroshio jet, may act as a barrier to the cross-gyre exchange of surface nutrients. *Bower et al.* [1985] used hydrographic surveys to investigate exchange across the Gulf Stream and concluded it acts largely as a barrier in upper waters. Reaching a similar

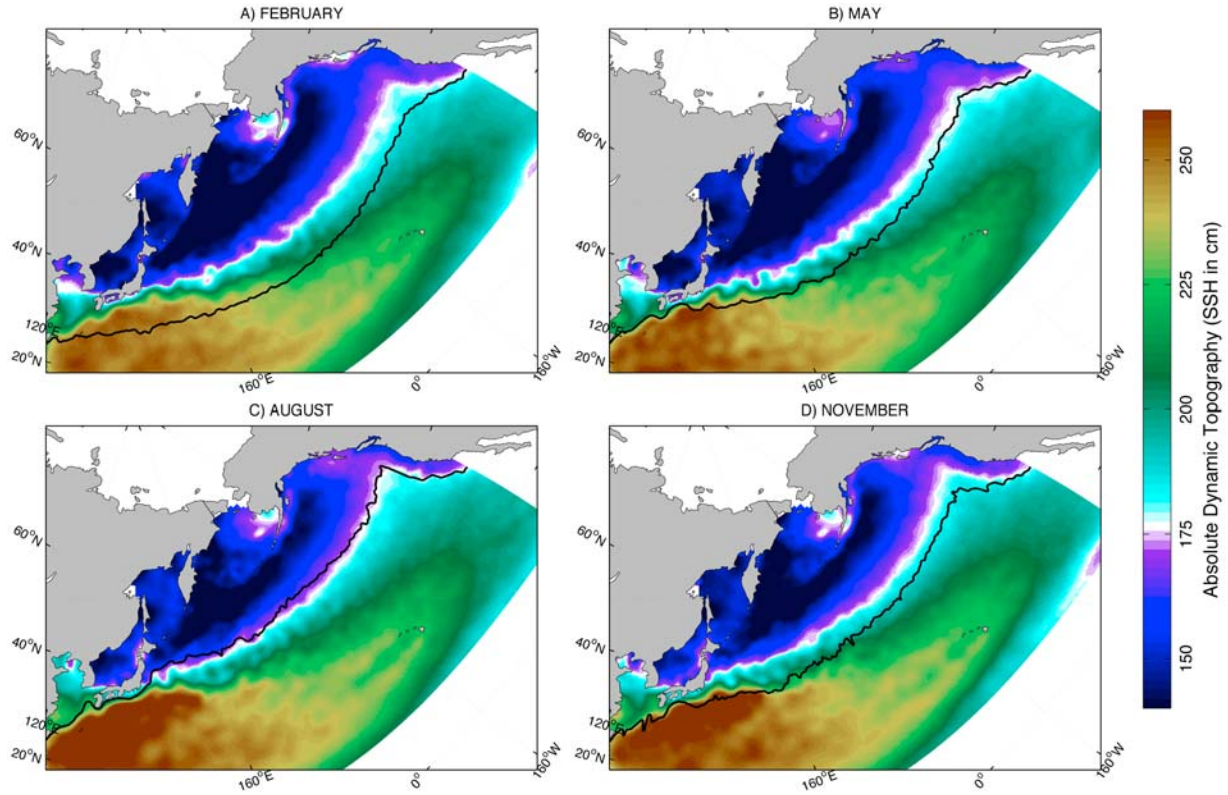

Figure 2. TZCF (black line, as in Figure 1) overlain on SSH in (a) February, (b) May, (c) August, and (d) November. Dynamic height data shown are monthly climatologies from 1999 to 2008, from an Archiving, Validation, and Interpretation of Satellite Oceanographic data (AVISO) product using data from Topex/Poseidon, ERS-1, ERS-2, Jason-1, and Envisat altimeters. The 175 cm SSH contour, chosen as an approximation of the gyre-gyre boundary because it does not join the recirculation pattern of either gyre, is highlighted in white.

conclusion, *Lozier and Riser* [1990] found that in a modeled ocean, the strong potential vorticity gradient at the center of the east-west jet acts as a boundary to surface exchange between gyres. Given this apparent dynamical barrier, we might expect the maximum chlorophyll gradient marked by the TZCF to lie along the gyre-gyre boundary separating the relatively eutrophic and oligotrophic nutrient regimes. To investigate this hypothesis, we compare the location of the TZCF to that of the gyre-gyre boundary, using sea surface dynamic height to indicate geostrophic circulation patterns.

[9] A superposition of the TZCF on the sea surface dynamic height field reveals strong seasonal differences in their relationship (Figure 2). During summer (August) the location of the TZCF is as predicted, coinciding remarkably well with the gyre-gyre boundary, approximated here by the 175 cm dynamic height contour separating the two gyres. In contrast, during the winter (February), the TZCF ceases to show any relation to the gyre structure, cutting across the dynamic height front and lying well to its south, in the northern reaches of the subtropical gyre. Fall (November) and spring (May) are transitional seasons in which the TZCF lies between the summer and winter extremes. As Figure 2 reveals, the TZCF appears constrained by the gyre-gyre boundary in summer and unconstrained by the gyre boundary in winter.

[10] The seasonal relationship between the TZCF and the gyre structure gives insight into possible forcing mechanisms. The disconnect between the TZCF and the gyre boundary in the winter suggests that expansion and contraction of the subarctic and subtropical gyres cannot be the cause of the seasonality in the TZCF, as previously suggested [*Chai et al.*, 2003]. It simultaneously indicates that the low-latitude winter TZCF position in the northern reaches of the subtropical gyre must be sustained by a nutrient source other than upwelling, as the subtropical gyre is characterized by downwelling. Furthermore, the southward winter migration of the TZCF must be forced via a mechanism that can operate throughout the region of the gyre-gyre boundary that it crosses. Sections 2.2 and 2.3 investigate two such candidates: vertical mixing and the horizontal advection of nutrients.

2.2. Vertical Mixing

[11] Deeper winter mixing as seasonal thermal stratification disappears is often thought to be a source of increased nutrients to surface waters, and has been suggested as a possible nutrient source to the wintertime TZCF in the subtropical gyre [*Glover et al.*, 1994; *Chai et al.*, 2003]. To examine this possibility, we compare the seasonal mixed layer depth (MLD) to that of the nitracline.

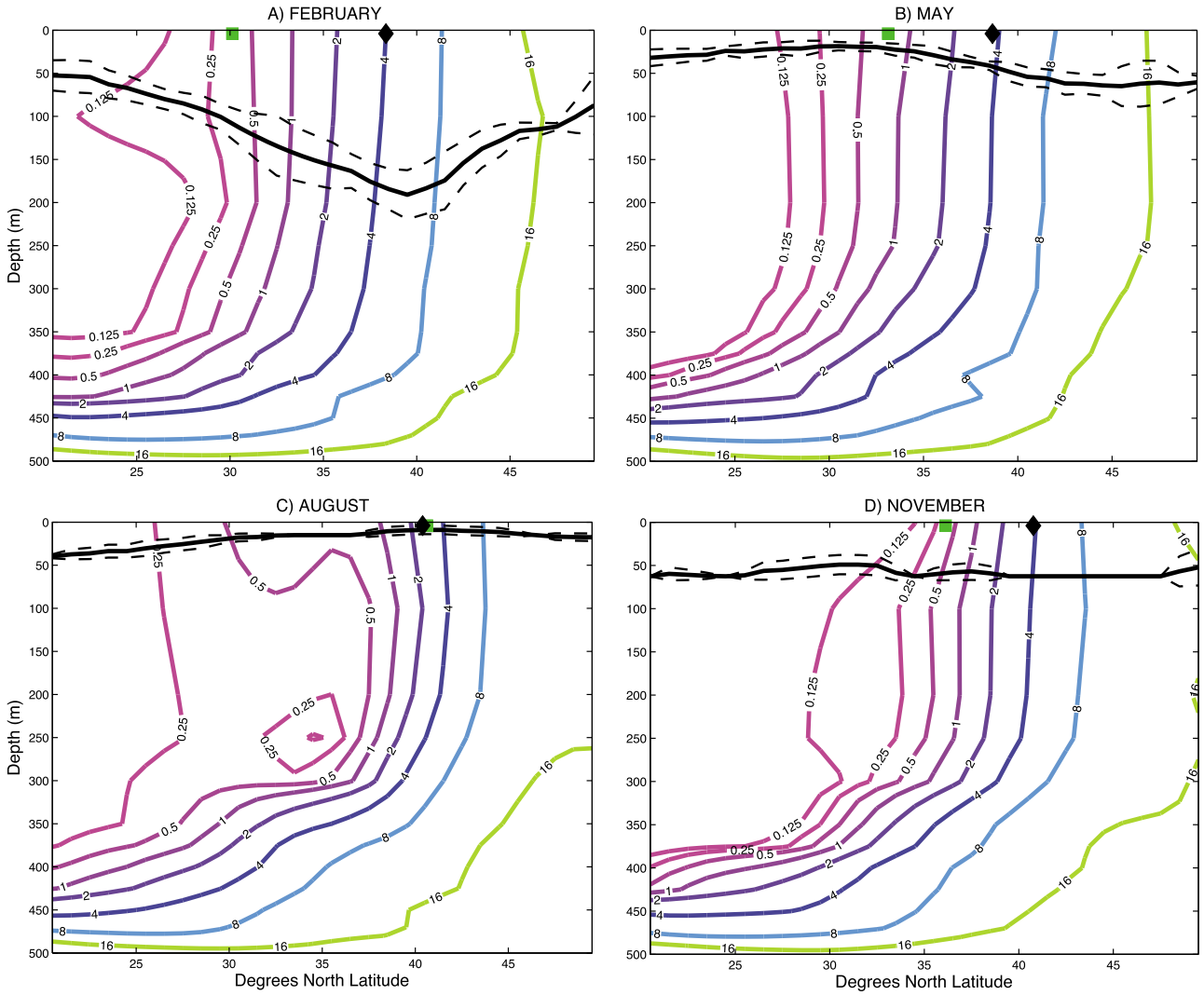

Figure 3. Nitrate profiles for (a) February, (b) May, (c) August, and (d) November. Monthly climatological nitrate data are from WOA05 in mmol m^{-3}, contoured on a log scale. MLD (horizontal black line) shown is the depth at which σ_θ increases by 0.125 from the surface value; σ_θ is derived from WOA05 gridded climatological temperature and salinity values [*Locarnini et al.*, 2006; *Antonov et al.*, 2006]. Dotted black lines flanking MLD indicate +/−1 standard deviation. Black diamonds indicate monthly mean latitude of 175 cm SSH contour (as in Figures 2a–2d). Green squares indicate monthly mean TZCF latitude (as in Figures 1a–1d). All data values are zonal averages from 160°E to 160°W, chosen to span the width of the Pacific while excluding gyre edges.

[12] Mixed layer depths and nitrate profiles are shown seasonally for comparison in Figure 3. All seasons show high values of nitrate in the subpolar gyre, low values in the subtropical, and the nitrate front between the two in the North Pacific transition zone. The MLD changes seasonally as expected, shoaling in the summer and deepening in the winter. The large latitudinal migration of the TZCF is also shown in Figure 3, along with the small seasonal variability in the location of the gyre-gyre boundary.

[13] Summer (Figure 3c) shows the TZCF coincident with the gyre-gyre boundary, as approximated by the 175 cm sea surface height (SSH) contour shown earlier in Figure 2c. The subsurface nitrate front between the subpolar and subarctic gyres is most defined in this season, outcropping at the surface around 40°N, in the region of the TZCF. The seasonal mixed layer depth here is shallow, 25 m or less, but remains rich in nutrients to the north from upwelling in the subpolar gyre. The summer TZCF thus lies explicably along the gyre-gyre boundary.

[14] In contrast the winter (Figure 3a) produces deeper mixed layers, reaching depths of 100–150 m in the TZCF region, and up to 200 m in the seasonal low stability gap from about 37°N to 42°N, described by *Roden* [1991]. However, the winter MLD remains too shallow to be the primary source of nutrients to the TZCF, as the nitracline remains far below it (another 250–300 m).

[15] While the data presented in Figure 3 discount vertical mixing as the primary nutrient source to the winter TZCF,

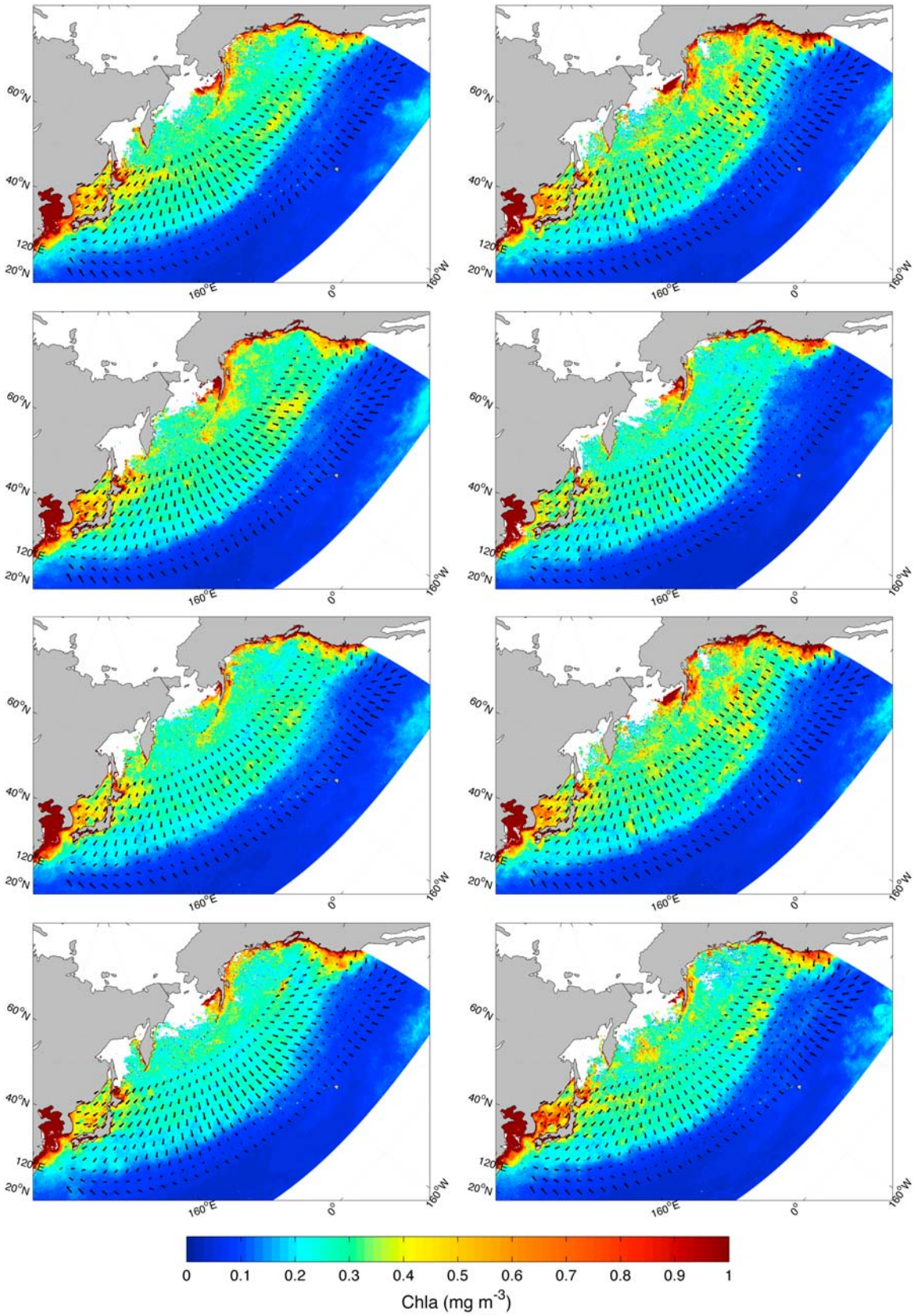

Figure 4. Winter (DJF) chlorophyll *a* values (mg m^{-3}) from SeaWiFS for (left) 2000–2003 and (right) 2004–2007. Vectors are horizontal Ekman transports, calculated as $\mathbf{u}_{Ek} = \tau_y/\rho f$ and $\mathbf{v}_{Ek} = -\tau_x/\rho f$ in $m^2\ s^{-1}$, where τ is the wind stress. Wind velocity data are from the QuikSCAT scatterometer, distributed by the NASA Physical Oceanography Distributed Active Archive Center.

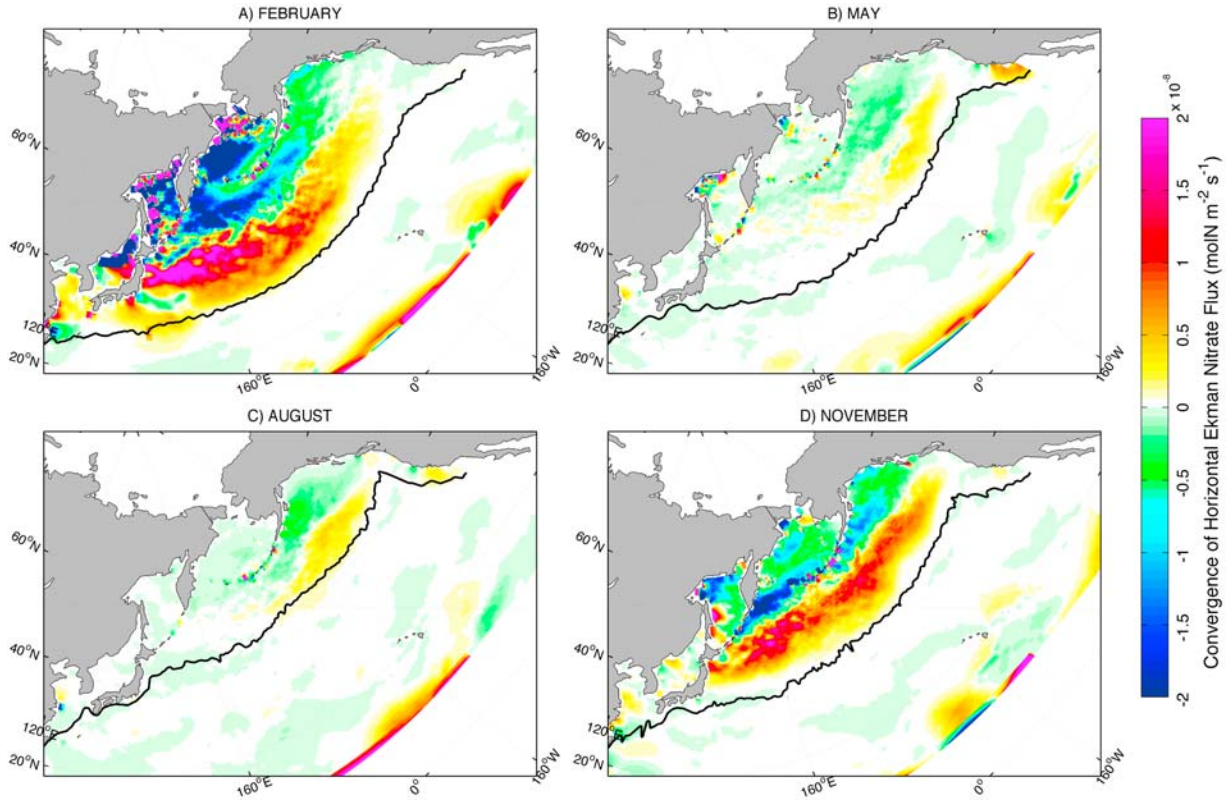

Figure 5. TZCF (black line, as in Figure 1) overlain on the convergence of the horizontal Ekman nitrate flux (mol N m^{-2} s^{-1}) in (a) February, (b) May, (c) August, and (d) November.

they also reinforce our earlier conclusion that the seasonal expansion and contraction of the gyres does not drive the TZCF migration. Though the gyre-gyre boundary shifts south by a few degrees latitude in the winter, the TZCF shifts disconnectedly, by a much larger 10° latitude. Finding no support in the data for these first two hypotheses, we next look to horizontal advection as a potential wintertime nutrient source.

2.3. Horizontal Advection

[16] Neither upwelling nor deep winter mixing, paradigms of nutrient supply in oceanography, explain the existence of the winter TZCF in the subtropical gyre. In the absence of a vertical nutrient supply, we investigate a horizontal supply. Several studies have found nutrients supplied by horizontal advection. *Palter et al.* [2005] found horizontal advection to significantly impact the nutrient reservoir beneath the North Atlantic subtropical gyre. *Williams and Follows* [1998] found that the horizontal Ekman transport of nutrients from the north, across the gyre-gyre boundary, supported a significant portion of primary productivity in the northern reaches of the North Atlantic subtropical gyre. On the California coast, variations in southward Ekman transport were found to explain 50–60% of variance in zooplankton abundance [*Wickett*, 1967]. Here we investigate the role of horizontal advection, and Ekman transport in particular, in the supply of nutrients to the North Pacific transition zone.

[17] Ekman transport moves surface waters to the right of the Westerlies, carrying waters southward throughout the North Pacific transition zone region (Figure 4). This southward flow occurs in the band extending from the southern reaches of the subarctic gyre at the northern edge of the Westerlies, across the gyre-gyre boundary where the Westerlies are strongest, and into the northern reaches of the subtropical gyre at the southern edge of the Westerlies.

[18] We find a compelling correlation between horizontal Ekman transport and the location of the TZCF in wintertime, when the winds are strongest. Figure 4 shows horizontal Ekman transport overlain on the winter chlorophyll field for eight sequential years. In each year, the southern extent of the Ekman transport predicts well the southern extent of the higher chlorophyll signature that is essentially the TZCF.

[19] This apparent correlation between horizontal Ekman transport and the winter TZCF position is consistent with the suggestion by *Bograd et al.* [2004] that equatorward advection of nutrient-rich waters from the north may sustain chlorophyll in the northern subtropical gyre during winter. However, in order for Ekman transport to have an impact in the region, the nutrients must converge. Assuming nitrogen to be the limiting nutrient [*Lewis et al.*, 1986], a convergence of the Ekman transport of nitrate could mechanistically explain the observed correlation in Figure 4.

[20] Estimates of the horizontal Ekman supply of nitrate to the North Pacific transition zone are made using methods similar to those used by *Williams and Follows* [1998]. The depth-integrated horizontal Ekman flux of nitrate ($\mathbf{u}_{HEk}NO_3$) is calculated using the Ekman transports (m^2 s^{-1}) shown in

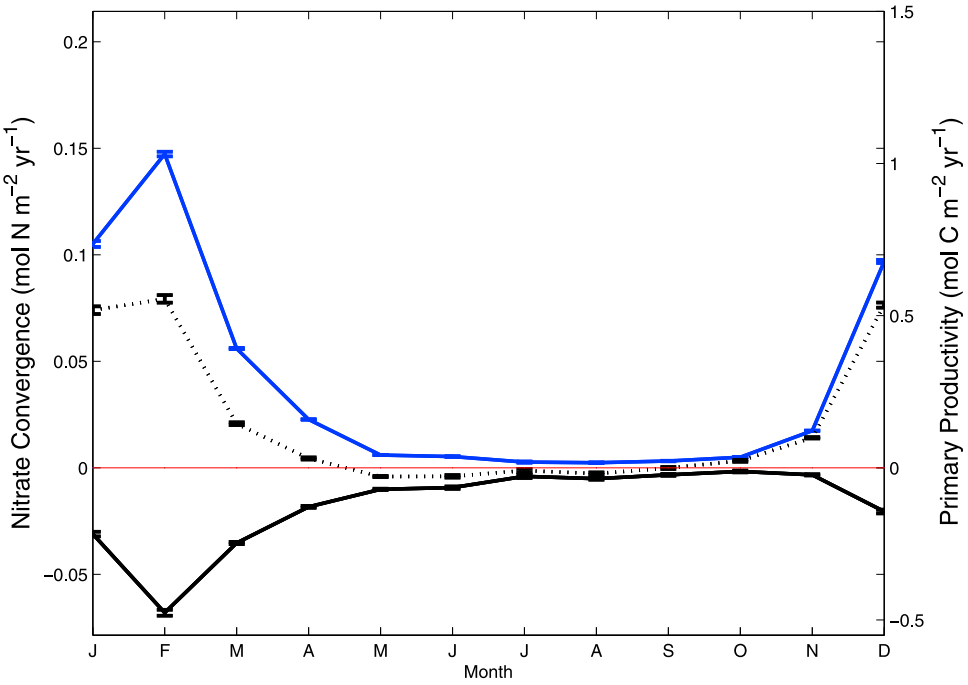

Figure 6. Transition zone nitrogen and carbon. Convergence of Ekman (blue), geostrophic (solid black), and Ekman plus geostrophic (black dotted) nitrate fluxes to the North Pacific transition zone in mol N m^{-2} y^{-1} (left axis). Corresponding new primary productivity supported by the nitrate in mol C m^{-2} y^{-1} (right axis). A Redfield ratio of 105C:15N translates between the left and right axes. Error bars indicate 1 standard deviation, calculated using a Monte Carlo simulation taking the standard deviations of geostrophic currents in the Kuroshio region to be 22% of the mean [*Kakinoki et al.*, 2008], the Ekman transports to be 25% of the mean [*Stoll et al.*, 1996], and standard deviations of nitrate to vary monthly, with the median at 41% of the mean (WOA05). Geostrophic velocities used in calculating nitrate convergence are from AVISO, derived from SSH. All values are calculated for the transition region as defined in section 3.

Figure 4 and the monthly mean nitrate concentration (mmol m^{-3}) in the Ekman layer. Mean Ekman layer nitrate is calculated using WOA05 monthly climatological nitrate profiles averaged over Ekman depths ranging from 10 to 70 m, calculated from QuikSCAT winds.

[21] Figure 5 shows the convergence of the horizontal Ekman nitrate flux ($-\nabla \cdot \mathbf{u}_{\mathrm{H}Ek}NO_3$) for each season, overlain with the TZCF position. In each season, the southern extent of the high-chlorophyll region, marked by the TZCF, is determined by the southernmost extent of the convergence of the southward Ekman nitrate flux. This relationship is particularly strong in winter months with high winds (November and February). The relationship holds in the months surrounding summer (May and August), though weaker winds result in less nutrient convergence. We note that the TZCF position expectedly correlates with this flux of nitrate (Figure 5), rather than the standing stock of nitrate (Figure 3).

[22] The convergence of the horizontal Ekman flux of nitrate offers a mechanistic explanation for the location of the winter TZCF in an otherwise puzzling location: a convergent, downwelling zone, over a deep nutricline untapped by deep winter mixing. This explains the observation by *Bograd et al.* [2004] that the TZCF is coincident with the region of maximum negative wind stress curl (WSC) in the winter. Westerly winds north of the region of maximum negative WSC drive the southward Ekman transport of surface waters, carrying nutrients across the gyre boundary and forcing the TZCF southward into the northern reaches of the subtropical gyre.

[23] Though Figures 4 and 5 suggest Ekman transport is important in driving the winter location of the TZCF, Ekman flow accounts for only a small portion of total surface flow (9–16% from summer to winter) in the NPTZ. The remainder of this surface flow is geostrophic. As the convergence of nitrate due to the total surface flow ultimately determines nutrient availability, we evaluate this next in Figure 6.

[24] Figure 6 (left axis) compares the Ekman and geostrophic contributions of nitrate to the NPTZ. In all months, Ekman transport converges nitrate, while geostrophic flow removes it. In the high-wind months of October–April, the convergence of Ekman nitrate fluxes dominates that of the geostrophic flow, supplying the northern reaches of the subtropical gyre with nitrate. Thus Figure 6 reveals that Ekman transport forces the winter TZCF migration through nutrient convergences, despite its small magnitude relative to geostrophic flows. Next we investigate the relative importance of these nutrient sources in the transition zone.

3. Quantifying Nutrient Sources

[25] Here we quantify the relative importance of Ekman-driven nitrate fluxes via the conservation equation. The

conservation of nitrate within the Ekman layer can be expressed as

$$\left.\frac{\partial NO_3}{\partial t}\right|_{D_{Ek}}^{surface} = -\nabla \cdot \mathbf{u}_{HEk} NO_3 - \nabla \cdot \mathbf{u}_{Geo} NO_3 - \frac{\partial wNO_3}{\partial z} + k_H \nabla_H^2 NO_3 + k_V \frac{\partial^2 NO_3}{\partial z^2} + SMS,$$

where NO_3 is the nitrate concentration, D_{Ek} is the depth of the Ekman layer, u_{HEk} is the horizontal Ekman transport, u_{Geo} is the geostrophic transport, and k_H and k_V are the horizontal and vertical eddy diffusivity coefficients, respectively. Local, temporal changes in the Ekman layer nitrate concentration ($\partial NO_3/\partial t$) can result from the processes on the right hand side of the equation: (1) convergence of the horizontal Ekman nitrate flux, (2) convergence of the geostrophic nitrate flux, (3) vertical convergence of nitrate, (4) horizontal mixing of nitrate, (5) vertical mixing of nitrate, and (6) biological sources and sinks of nitrate.

[26] 1. The average annual convergence of nitrate in the transition zone due to horizontal Ekman transport is approximately 9.3×10^{-10} mol N m^{-2} s^{-1} (0.03 mol N m^{-2} y^{-1}). February sees the strongest convergence rates of 0.15 mol N m^{-2} y^{-1}, while August sees the weakest of roughly 2.0×10^{-3} mol N m^{-2} y^{-1} (Figure 6). These estimates are averaged over the transition zone region defined here as: 30°N–40°N (from the climatological southern extent of the TZCF to the northern extent), and 150°E–130°W (the zonal extent of the Pacific basin, cutting off boundary regions).

[27] 2. The average annual geostrophic flux of nitrate in the transition zone diverges rather than converges, at a rate of 6.4×10^{-10} mol N m^{-2} s^{-1} (0.02 mol N m^{-2} y^{-1}). This divergence of nitrate is strongest in February at an estimated rate of 0.07 mol N m^{-2} y^{-1}, notably removing nitrate more slowly than Ekman convergence supplies it (Figure 6). Similar to the Ekman convergence of nitrate, the geostrophic divergence of nitrate is smallest in summer months.

[28] 3. The vertical advection term, $\partial wNO_3/\partial z$, removes nitrate from the system as well. The convergence of the Ekman transport over the spatial domain of this study produces a downward vertical nitrate flux at the base of the Ekman layer, leading to a sink for the nitrate in the upper waters ($\partial wNO_3/\partial z > 0$).

[29] 4. The horizontal mixing term, $k_H \nabla_H^2 NO_3$, can be scaled as $k_H(\Delta_x NO_3/L_x^2 + \Delta_y NO_3/L_y^2)$. An optimal k_H of 500 m^2 s^{-1} is listed by *Visbeck et al.* [1997] for the Ekman convergence zone in the North Pacific, and ΔNO_3 can be calculated from WOA05 data for the transition zone region. Using k_H = 500 m^2 s^{-1}; L_x = 5000 km with $\Delta_x NO_3 = -2 \times 10^{-6}$ mol NO_3 m^{-3}; L_y = 1000 km with $\Delta_y NO_3$ = 0.003 mol NO_3 m^{-3}; and integrated over an Ekman depth approximated at 40 m, the change in nitrate in the Ekman layer due to horizontal mixing is approximately 6×10^{-11} mol N m^{-2} s^{-1}.

[30] 5. The vertical mixing term $k_V(\partial^2 NO_3/\partial z^2)$ can be scaled as $k_V(\Delta NO_3/D^2)$. Using $k_V = 10^{-4}$ m^2 s^{-1}, used by *Kimura et al.* [2000] for the Kuroshio Extension region; $\Delta NO_3 = 1.1 \times 10^{-5}$ mol N m^{-3} for D = 250 m, calculated from the WOA05 nitrate profile data in the transition zone box; and integrated over an Ekman depth approximated at 40 m, the contribution of vertically mixed nitrate to the transition zone is approximately 7×10^{-13} mol N m^{-2} s^{-1}.

[31] Summarizing the physical terms, the only oceanic processes that can supply nutrients to the transition zone are convergence of the horizontal Ekman flux of nitrate (1), horizontal mixing of nitrate (4), and vertical mixing of nitrate (5). Of these, term 1 dominates. Convergence of the horizontal Ekman flux of nitrate, approximately 9×10^{-10} mol N m^{-2} s^{-1}, dominates nitrate supplied through horizontal mixing, approximately 6×10^{-11} mol N m^{-2} s^{-1}. Both of these horizontal processes clearly dominate vertical mixing, approximately 7×10^{-13} mol N m^{-2} s^{-1}.

[32] 6. Finally, physical processes are not the only potential sources of nitrate; biological sources may also make a contribution. Rates of biological input via N_2 fixation in the North Pacific transition zone are unavailable, but several authors have estimated N_2 fixation in the oligotrophic subtropical North Pacific. *Karl et al.* [1997] report fixation rates of 0.034 mol N m^{-2} y^{-1} at ocean station ALOHA. However, this estimate is based in part on *Trichodesmium spp.* fixation rates and abundances, whereas *Trichodesmium* may be limited to waters > 20°C [*Dore et al.*, 2002] and the TZCF region is cooler, ~18°C [*Bograd et al.*, 2004]. Thus, the N_2 fixation rate in the transition zone might reasonably be expected to be less. *Dore et al.* [2002] report a range of fixation rates from a low of 0.031 mol N m^{-2} y^{-1} to a high of 0.084 mol N m^{-2} y^{-1} at station ALOHA over an 11 year period. In each of these studies nitrogen fixation is estimated to account for up to 50% of total exported nitrogen. *Wilson et al.* [2008] likewise found N_2 fixation important, as *Richelia* in part controls a recurring late summer chlorophyll bloom in the subtropical North Pacific, south of the TZCF. These nitrogen fixation rates estimated for oligotrophic North Pacific waters are of a similar magnitude to our estimates of the horizontal Ekman advection of nitrate to the transition zone, estimated above as 0.03 mol N m^{-2} y^{-1}.

[33] A scale analysis of the conservation equation for nitrate has quantitatively shown the convergence of the horizontal Ekman flux of nitrate to be the primary oceanic process providing nutrients to the North Pacific transition zone. Next we consider the contribution of this nutrient source to estimated new productivity, with the consideration that biological N_2 fixation may also play a notable role.

4. Contribution of Horizontal Ekman Advection to New Primary Productivity

[34] The current paradigm for primary productivity (PP) is that while regenerated production is supplied by recycled organic matter within the surface of the ocean, new primary productivity (NPP) is fueled by external nutrients upwelled or mixed upwards from below the thermocline [*Sarmiento and Gruber*, 2006]. Transition zone waters appear to defy this paradigm; rather than vertical nutrient sources driving new production, horizontal advection controls nutrient delivery. Indeed, the following estimates show that horizontal Ekman-advected nitrogen can support up to 40% of new primary productivity annually, and the majority of new primary productivity in winter in the North Pacific transition zone.

[35] Nitrate inputs to the transition zone are shown on the left axis of Figure 6, as discussed previously. The right axis shows the corresponding primary productivity rates sup-

ported by these advective sources: convergence of horizontal Ekman nitrate flux (input), divergence of geostrophic nitrate flux (removal), and their sum.

[36] The portion of new productivity supported by these advective fluxes varies significantly from season to season. In winter, horizontal Ekman transport oversupplies the transition zone with nitrate, while the geostrophic flow removes it. The sum of these sources averaged December–March contributes approximately 0.06 mol N m^{-2} y^{-1} to the region, translating to 0.44 mol C m^{-2} y^{-1} of productivity (Figure 6). Over this same time period new productivity is estimated at 0.41 mol C m^{-2} y^{-1}, using products from the Behrenfeld CbPM Model [*Behrenfeld et al.*, 2005] and an *f* ratio of 0.13 for transition zone waters [*Eppley and Peterson*, 1979]. Errors associated with NPP estimates should be noted: the Behrenfeld CbPM model estimated PP rates from 0.82 to 1.13 times measured in situ rates in the tropical Pacific [*Friedrichs et al.*, 2009]; subsequently using an *f* ratio to scale from PP to NPP introduces additional error. Nevertheless, it is clear that the horizontal Ekman flux of nitrate supports the majority of new production in the transition zone in the wintertime.

[37] In contrast, the highest rates of production occur in summer, with new productivity in June, July, and August (JJA) estimated at 1.76 mol C m^{-2} y^{-1} (Behrenfeld CbPM), yet the Ekman contribution of nitrate is essentially none and the geostrophic flow continues to remove it (Figure 6). Instead, this high summer productivity rate may be explained in part by N_2 fixation. *Dore et al.* [2002] found that N_2 fixation accounted for 36–69% of new productivity in the oligotrophic subtropical gyre, with the highest rates in May–August and the lowest in November–January. We found that winter productivity is forced almost entirely by the convergence of horizontal Ekman nitrate transport; we propose that N_2 fixation may fill in the gap in the summer, but leave this as a hypothesis for further studies.

[38] Our estimates for annual productivity supported by the horizontal Ekman nitrate supply to the North Pacific transition zone are in concert with similar estimates made for the transition zone waters of the North Atlantic. *Williams and Follows* [1998] estimated that horizontal Ekman fluxes of nitrate support 0.4 to 0.6 mol C m^{-2} y^{-1} of new production on the northern flank of the North Atlantic subtropical gyre. They compare this to the 1 mol C m^{-2} y^{-1} in estimated new production for the region, and conclude that on an annual time scale the horizontal advection of nitrate is a significant source of nutrients in transitional waters. We estimate here that the annual horizontal Ekman supply of nitrate to the North Pacific transition zone supports approximately 0.2 mol C m^{-2} y^{-1} of new production. (The 0.2 mol C m^{-2} y^{-1} figure of new production reported here is the mean from January to December. The figure *Williams and Follows* [1998] reported instead used the sum of October–April divided by 12 as their lower bound, and the mean from October to April as the higher bound. Calculated in the manner of Williams and Follows, the annual horizontal Ekman supply of nitrate to the NPTZ supports 0.2 to 0.4 mol C m^{-2} y^{-1} of new production.)

[39] We compare this to the total estimated new production of 0.5 to 0.8 mol C m^{-2} y^{-1} from the Behrenfeld CbPM for the region, and find that horizontal advection supports approximately 25–40% of new production annually. In the transition zone waters of both the North Pacific and the North Atlantic, the horizontal Ekman flux of nitrate plays a significant role in supporting new primary productivity.

5. Summary and Conclusion

[40] Our motivation to understand the physical dynamics driving the 1000 km seasonal migration of the TZCF within the North Pacific transition zone stems from its potential impact on the distribution and survival of species, both commercial and endangered, that use this habitat for migration and foraging [*Polovina et al.*, 2001; *Chavez et al.*, 2003; *Bograd et al.*, 2004]. The schematic in Figure 7 summarizes our model for the seasonal forcing of the TZCF.

[41] In summer the TZCF lies at its most northerly position, located at the gyre-gyre boundary. Chlorophyll lies within the bounds of the subpolar gyre, supported with nutrients via upwelling from below [*Reid*, 1962]. Weak winds result in small southward Ekman transports that converge nitrate in the southern portion of the subpolar gyre. This is consistent with the expectation that the gyre-gyre boundary acts as barrier to cross-gyre exchange [*Bower et al.*, 1985; *Lozier and Riser*, 1990].

[42] Starting in fall and at its most extreme in winter, the TZCF moves southward. High winds result in large southward Ekman transports that carry nutrients across the gyre boundary, converging nitrate in the northern reaches of the subtropical gyre. The TZCF lies at the southernmost extent of this convergence. This mechanism explains the observation by *Bograd et al.* [2004] that the wintertime TZCF is located on the region of maximum negative WSC. *Williams and Follows* [1998] similarly determined that southward Ekman fluxes converge nitrate in the northern flanks of the subtropical gyre in the North Atlantic. Also in support, *Brambilla and Talley* [2006] found Ekman transports affect intergyre flux despite the gyre-gyre boundary, concluding that southward mean Ekman velocities inhibited synthetic drifters from crossing into the subpolar gyre from the North Atlantic subtropical gyre.

[43] Completing the annual cycle, the TZCF begins its retreat to higher latitudes in spring. Winds die down, easing off the Ekman transport nutrient delivery. By summer, the TZCF has returned to its northernmost summertime position.

[44] The analyses here do not support previous hypotheses for the winter TZCF location. The deep winter mixed layer lies well above the nutricline in the North Pacific transition zone, unable to access the nutrient-rich waters of the deep. And while the gyres show a small seasonal expansion and contraction, this does not match the shift of the TZCF in magnitude or location. Instead, we find the latitude of the TZCF shows an inverse relationship to the magnitude of the wind stress, its migration controlled by a combination of the convergence of Ekman nitrate fluxes and the gyre-gyre boundary (Figure 7).

[45] A scaling analysis showed the convergence of the horizontal Ekman nitrate fluxes to be the dominant physical source of nutrients to the transition zone. These nutrients support up to 40% of new production in the region annually, and almost all of new production in the winter. This nutrient source disappears in the region in summer, when we postulate that N_2 fixation may instead support the majority of

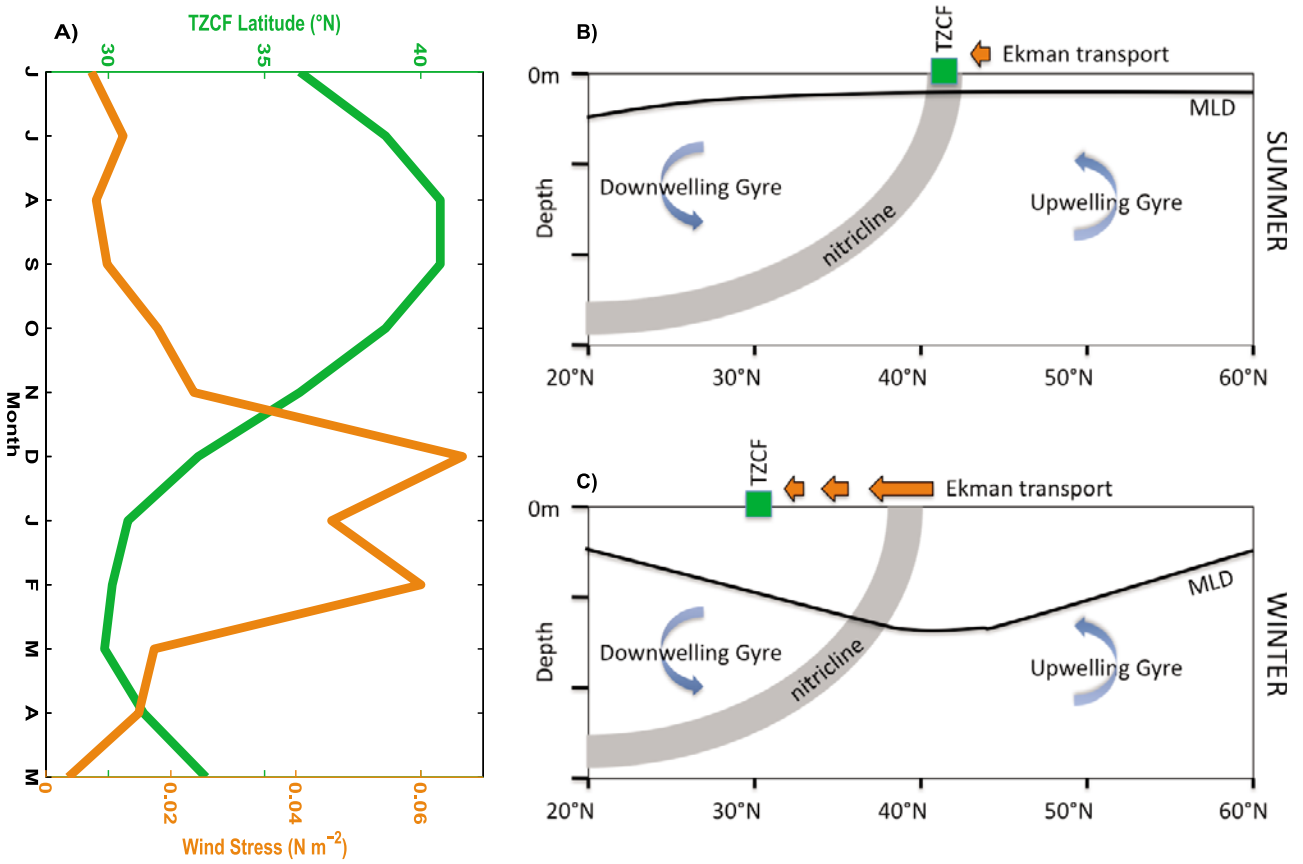

Figure 7. Model of dominant seasonal drivers of the TZCF. (a) The TZCF latitude shows an inverse relation to the magnitude of the wind stress (QuikSCAT scatterometer monthly climatologies). (b) In summer, the TZCF sits on the gyre boundary. Nutrients are upwelled from below to the subarctic gyre. Low winds are insufficient for Ekman transports to carry these nutrients south across the gyre-gyre boundary, resulting in a high-latitude TZCF. (c) In winter, the TZCF sits south of the gyre boundary, at the southern extent of the convergence of southward horizontal Ekman nitrate fluxes. High winds create Ekman transports that overcome the gyre boundary, carrying nitrate into the northern reaches of the subtropical gyre, resulting in a low-latitude TZCF. The MLD remains too shallow to penetrate the nutricline, even in winter. The small seasonal shift of the gyre boundary is disconnected from the large seasonal shift of the TZCF.

summertime new production. However, this remains a question for future investigations.

[46] Finally, we return to the biological motivations of this investigation. Past studies have shown that variations in wind and wind-forced waters affect zooplankton distributions [*Wickett*, 1967; *Brodeur and Ware*, 1992], and are believed to have an impact on the distribution of fish as well [*Checkley et al.*, 1988; *Seckel*, 1988; *Hinz*, 1989]. The convergence of Ekman transports discussed herein may be a factor in concentrating zooplankton and other gelatinous organisms along the TZCF, resulting in a food web that supports higher trophic levels, as proposed by *Polovina et al.* [2001]. We have shown that winds force chlorophyll distribution in the North Pacific transition zone, and hope our findings will aid future investigations into the relationship between marine megafauna and the TZCF.

[47] **Acknowledgments.** Support for the work of J.M.A. provided by a National Defense Science and Engineering Graduate Fellowship (NDSEG). Support for the work of M.S.L. provided by the National Science Foundation (NSF). We thank R.T. Barber for helpful comments on this work.

References

Antonov, J. I., R. A. Locarnini, T. P. Boyer, A. V. Mishonov, and H. E. Garcia (2006), *World Ocean Atlas 2005*, vol. 2, *Salinity*, *NOAA Atlas NESDIS*, vol. 62, NOAA, Silver Spring, Md.

Behrenfeld, M. J., E. S. Boss, D. A. Siegel, and D. M. Shea (2005), Carbon-based ocean productivity and phytoplankton physiology from space, *Global Biogeochem. Cycles*, *19*, GB1006, doi:10.1029/2004GB002299.

Bograd, S. J., D. G. Foley, F. B. Schwing, C. Wilson, R. M. Laurs, J. J. Polovina, E. A. Howell, and R. E. Brainard (2004), On the seasonal and interannual migrations of the transition zone chlorophyll front, *Geophys. Res. Lett.*, *31*, L17204, doi:10.1029/2004GL020637.

Bower, A. S., H. T. Rossby, and J. L. Lillibridge (1985), The Gulf Stream: Barrier or blender?, *J. Phys. Oceanogr.*, *15*, 24–32, doi:10.1175/1520-0485(1985)015<0024:TGSOB>2.0.CO;2.

Brambilla, E., and L. D. Talley (2006), Surface drifter exchange between the North Atlantic subtropical and subpolar gyres, *J. Geophys. Res.*, *111*, C07026, doi:10.1029/2005JC003146.

Brodeur, R. D., and D. M. Ware (1992), Long-term variability in zooplankton biomass in the subarctic Pacific Ocean, *Fish. Oceanogr.*, *1*(1), 32–38, doi:10.1111/j.1365-2419.1992.tb00023.x.

Chai, F., M. Jiang, R. T. Barber, R. C. Dugdale, and Y. Chao (2003), Interdecadal variation of the transition zone chlorophyll front: A physical-biological model simulation between 1960 and 1990, *J. Oceanogr.*, *59*, 461–475, doi:10.1023/A:1025540632491.

Chavez, F. P., J. Ryan, S. E. Lluch-Cota, and C. M. Niquen (2003), From anchovies to sardines and back: Multidecadal change in the Pacific Ocean, *Science*, *299*, 217–221, doi:10.1126/science.1075880.

Checkley, D. M., S. Raman, G. L. Maillet, and K. M. Mason (1988), Winter storm effects on the spawning and larval drift of a pelagic fish, *Nature*, *335*, 346–348, doi:10.1038/335346a0.

Dore, J. E., J. R. Brum, L. M. Tupas, and D. M. Karl (2002), Seasonal and interannual variability in sources of nitrogen supporting export in the oligotrophic subtropical North Pacific Ocean, *Limnol. Oceanogr.*, *47*(6), 1595–1607.

Eppley, R. W., and B. J. Peterson (1979), Particulate organic matter flux and planktonic new production in the deep ocean, *Nature*, *282*, 677–680, doi:10.1038/282677a0.

Friedrichs, M. A., et al. (2009), Assessing the uncertainties of model estimates of primary productivity in the tropical Pacific Ocean, *J. Mar. Syst.*, *76*, 113–133, doi:10.1016/j.jmarsys.2008.1005.1010.

Garcia, H. E., R. A. Locarnini, T. P. Boyer, and J. I. Antonov (2006), *World Ocean Atlas 2005*, vol. 4, *Nutrients (Phosphate, Nitrate, Silicate)*, *NOAA Atlas NESDIS*, vol. 64, NOAA, Silver Spring, Md.

Glover, D. M., J. S. Wroblewski, and C. R. McClain (1994), Dynamics of the transition zone in coastal zone color scanner-sensed ocean color in the North Pacific during oceanographic spring, *J. Geophys. Res.*, *99*, 7501–7511, doi:10.1029/93JC02144.

Hinz, V. (1989), Monitoring the fish fauna in the Wadden Sea with special reference to different fishing methods and effects of wind and light on catches, *Helgol. Meeresunters.*, *43*, 447–459, doi:10.1007/BF02365903.

Inagake, D., H. Yamada, K. Segawa, M. Okazaki, A. Nitta, and T. Itoh (2001), Migration of young bluefin tuna, *Thunnus orientalis* Temminck et Schlegel, through archival tagging experiments and its relation with oceanographic conditions in the western North Pacific, *Bull. Natl. Res. Inst. Far Seas Fish.*, *38*, 53–81.

Kakinoki, K., S. Imawaki, H. Uchida, H. Nakamura, K. Ichikawa, S. Umatani, A. Nishina, H. Ichikawa, and M. Wimbush (2008), Variations of Kuroshio geostrophic transport south of Japan estimated from long-term IES observations, *J. Oceanogr.*, *64*, 373–384, doi:10.1007/s10872-008-0030-4.

Karl, D., R. Letelier, L. Tupas, J. Dore, J. Christian, and D. Hebel (1997), The role of nitrogen fixation in the biogeochemical cycling in the subtropical North Pacific Ocean, *Nature*, *388*, 533–538, doi:10.1038/41474.

Kimura, S., H. Nakata, and Y. Okazaki (2000), Biological production in meso-scale eddies caused by frontal disturbances of the Kuroshio Extension, *ICES J. Mar. Sci.*, *57*, 133–142, doi:10.1006/jmsc.1999.0564.

Lewis, M. R., W. G. Harrison, N. S. Oakey, D. Hebert, and T. Platt (1986), Vertical nitrate fluxes in the Oligotrophic Ocean, *Science*, *234*(4778), 870–873, doi:10.1126/science.234.4778.870.

Locarnini, R. A., A. V. Mishonov, J. I. Antonov, T. P. Boyer, and H. E. Garcia (2006), *World Ocean Atlas 2005*, vol. 1, *Temperature*, *NOAA Atlas NESDIS*, vol. 61, NOAA, Silver Spring, Md.

Lozier, M. S., and S. C. Riser (1990), Potential vorticity sources and sinks in a quasi-geostrophic ocean: Beyond western boundary currents, *J. Phys. Oceanogr.*, *20*, 1608–1627, doi:10.1175/1520-0485(1990)020<1608:PVSASI>2.0.CO;2.

Nichols, W. J., A. Resendiz, J. A. Sminoff, and B. Resendiz (2000), Transpacific migration of a loggerhead turtle monitored by satellite altimetry, *Bull. Mar. Sci.*, *67*(3), 937–947.

Palter, J. B., M. S. Lozier, and R. T. Barber (2005), The effect of advection on the nutrient reservoir in the North Atlantic subtropical gyre, *Nature*, *437*, 687–692, doi:10.1038/nature03969.

Polovina, J. J., D. R. Kobayashi, D. M. Parker, M. P. Seki, and G. H. Balazs (2000), Turtles on the edge: Movement of loggerhead turtles (*Caretta caretta*) along oceanic fronts, spanning longline fishing grounds in the central North Pacific, 1997–1998, *Fish. Oceanogr.*, *9*, 71–82, doi:10.1046/j.1365-2419.2000.00123.x.

Polovina, J. J., E. Howell, D. R. Kobayashi, and M. P. Seki (2001), The transition zone chlorophyll front, a dynamic global feature defining migration and forage habitat for marine resources, *Prog. Oceanogr.*, *49*, 469–483, doi:10.1016/S0079-6611(01)00036-2.

Polovina, J. J., G. H. Balazs, E. A. Howell, D. M. Parker, M. P. Seki, and P. H. Dutton (2004), Forage and migration habitat of loggerhead (*Caretta caretta*) and olive ridley (Lepidochelys olivacea) sea turtles in the central North Pacific Ocean, *Fish. Oceanogr.*, *13*(1), 36–51, doi:10.1046/j.1365-2419.2003.00270.x.

Ream, R., J. T. Sterling, and T. R. Loughlin (2005), Oceanographic features related to northern fur seal migratory movements, *Deep Sea Res. Part II*, *52*, 823–843, doi:10.1016/j.dsr1012.2004.1012.1021.

Reid, J. L. (1962), On circulation, phosphate-phosphorus content, and zooplankton volumes in the upper part of the Pacific Ocean, *Limnol. Oceanogr.*, *7*, 287–306.

Roden, G. I. (1991), Subarctic-subtropical transition zone of the North Pacific: Large-scale aspects and mesoscale structure, in *Biology, Oceanography, and Fisheries of the North Pacific*, edited by J. A. Wetherall, pp. 1–38, NOAA, Silver Spring, Md.

Sarmiento, J. L., and N. Gruber (2006), *Ocean Biogeochemical Dynamics*, Princeton Univ. Press, Princeton, N. J.

Seckel, G. R. (1988), Indices for mid-latitude North Pacific winter wind systems: An exploratory investigation, *GeoJournal*, *16*(1), 97–111, doi:10.1007/BF02626375.

Seki, M. P. (2005), *Transition zone, in Marine Ecosystems of the North Pacific*, pp. 201–209, N. Pac. Mar. Sci. Organ., Sidney, B. C., Canada.

Shaffer, S. A., Y. Tremblay, J. A. Awkerman, D. J. Anderson, D. A. Croll, B. A. Block, and D. P. Costa (2005), Comparison of light- and SST-based geolocation with satellite telemetry in free-ranging albatrosses, *Mar. Biol.*, *147*, 833–843, doi:10.1007/s00227-00005-01631-00228.

Simmons, S. E., D. E. Crocker, R. M. Kudela, and D. P. Costa (2007), Linking foraging behaviour of the northern elephant seal with oceanography and bathymetry at mesoscales, *Mar. Ecol. Prog. Ser.*, *346*, 265–275, doi:10.3354/meps07014.

Stoll, M. H. C., H. M. van Aken, H. J. W. de Baar, and C. J. de Boer (1996), Meridional carbon dioxide transport in the northern North Atlantic, *Mar. Chem.*, *55*, 205–216, doi:10.1016/S0304-4203(96)00057-6.

Visbeck, M., J. Marshall, T. Haine, and M. Spall (1997), Specification of eddy transfer coefficients in coarse-resolution ocean circulation models, *J. Phys. Oceanogr.*, *27*, 381–402, doi:10.1175/1520-0485(1997)027<0381:SOETCI>2.0.CO;2.

Weng, K. C., P. C. Castilho, J. M. Morrissette, A. M. Landiera-Fernandez, D. B. Holts, R. J. Schallert, K. J. Goldman, and B. A. Block (2005), Satellite tagging and cardiac physiology reveal niche expansion in salmon sharks, *Science*, *310*, 104–106, doi:10.1126/science.1114616.

Wickett, W. P. (1967), Ekman transport and zooplankton concentration in the North Pacific Ocean, *J. Fish. Res. Board Can.*, *24*(3), 581–594.

Williams, R. G., and M. J. Follows (1998), The Ekman transfer of nutrients and maintenance of new production over the North Atlantic, *Deep Sea Res. Part I*, *45*, 461–489.

Wilson, C., T. A. Villareal, N. Maximenko, S. J. Bograd, J. P. Montoya, and C. A. Schoenbaechler (2008), Biological and physical forcings of late summer chlorophyll blooms at 30°N in the oligotrophic Pacific, *J. Mar. Syst.*, *69*, 164–176, doi:10.1016/j.jmarsys.2005.09.018.

J. M. Ayers and M. S. Lozier, Department of Earth and Ocean Sciences, Nicholas School of the Environment, Duke University, Old Chemistry Building, Box 90227, Durham, NC 27708, USA. (jma40@duke.edu)